ACS APPLIED MATERIALS & INTERFACES

Letter

www.acsami.org

Locally Reinforced Polymer-Based Composites for Elastic Electronics

Randall M. Erb,[†,‡] Kunigunde H. Cherenack,[§,‡] Rudolf E. Stahel,[†] Rafael Libanori,[†] Thomas Kinkeldei,[⊥] Niko Münzenrieder,[⊥] Gerhard Tröster,[⊥] and André R. Studart*[,†]

[†]Complex Materials, Department of Materials and [⊥]Electronics Group, Department of Information Technology and Electrical Engineering, ETH-Zurich, Zurich, 8093, Switzerland

[§]Philips Corporate Technologies, 5.006 High Tech Campus 34, Eindhoven, 5656AE, The Netherlands

Supporting Information

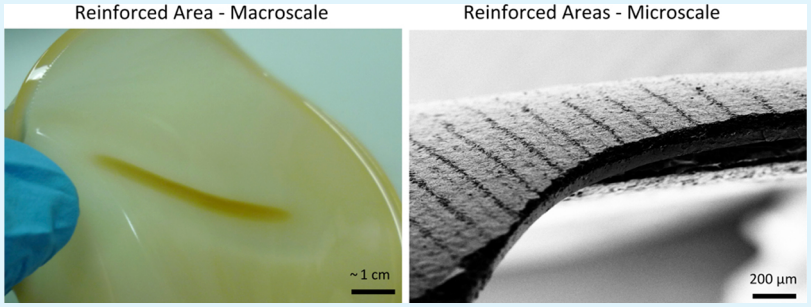

ABSTRACT: A promising approach to fabricating elastic electronic systems involves processing thin film circuits directly on the elastic substrate by standard photolithography. Thin film devices are generally placed onto stiffer islands on the substrate surface to protect devices from excessive strain while still achieving a globally highly deformable system. Here we report a new method to achieve island architectures by locally reinforcing polymeric substrates at the macro- and microscale using magnetically responsive anisotropic microparticles. We demonstrate that the resulting particle-reinforced elastic substrates can be made smooth enough for the patterning and successful operation of thin film transistors with transfer characteristics comparable to state-of-the-art devices

KEYWORDS: *elastic electronics, substrate engineering, composite materials, thin film transistors, magnetic ordering, discontinuous fiber composites*

Conformal electronics have a wide variety of applications ranging from smart textiles to flexible and elastic electronics. Elastic electronics applications include biological monitoring devices that conform to highly complex surfaces such as the surface of the brain,[1] or operate in mechanically active environments (e.g., attached to a beating heart).[2] Bioinspired elastic devices include "electronic eyes"[3] and sensor membranes mimicking human skin.[4] Elastic and flexible electronics have even recently been included in the Nokia Morph cell-phone prototype[5] and in displays.[6]

Three main methods of fabricating elastic electronic devices can be identified: (1) transfer processes where electronic circuits are fabricated on silicon wafers and printed onto elastic substrates,[1,2] (2) hybrid processes where conventional electronics are combined with elastic substrates,[7] and (3) fabrication of thin film devices (e.g., TFTs) directly on elastic substrates by standard cleanroom methods.[4] Unfortunately the mechanical and thermal properties of elastic polymeric substrates such as polydimethylsiloxane (PDMS) and standard metallic or ceramic device layers differ by several orders of magnitude.[4] For this reason, most photolithography approaches involve depositing stiff thin film layers (e.g., silicon nitride) onto elastic substrates, which are then patterned into islands for device placement, (Figure 1a). Adjacent device islands are connected using highly elastic interconnect lines consisting of metal or conducting organic material.[8] This prevents fragile devices from exposure to excessive strain while still resulting in a circuit that is globally highly deformable. However, such approaches result in an abrupt jump in material properties at the interface between the island and the rest of the substrate.[4] PDMS substrates for example exhibit elastic modulus of a few MPa, which is 5 orders of magnitude lower than that of silicon nitride. This results in high localized stress gradients, ultimately leading to early circuit failure.

A different way to approach this issue is to locally tune the mechanical properties of the elastic substrate itself to achieve a gradual transition between stiffer and softer regions. Lacour et al. described a technique to adjust the elastic modulus (E) of silicone membranes from 0.8 to 4 MPa by tuning the local cross-linking density using photolithography[9] to achieve a spatial resolution of 100 μm.

Instead, hierarchical reinforcement of homogeneous flexible substrates with inorganic nano- and microplatelets has been

Received: March 22, 2012
Accepted: June 7, 2012
Published: June 7, 2012

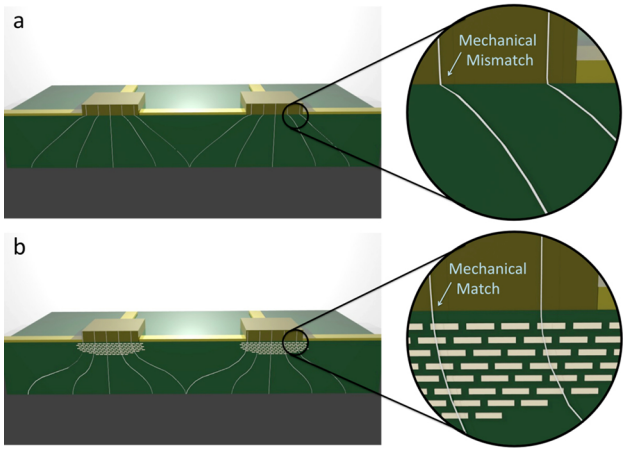

Figure 1. Expected strain profiles for rigid subcircuit islands fabricated on (a) pure polymers and (b) locally reinforced polymers. Insets depict mechanical matching occurring only at the interface of the locally reinforced polymers. Panel a was adapted with permission from ref 4. Copyright 2005 IEEE.

shown to enable tuning of the elastic modulus of elastomeric polyurethane from 200 to 7000 MPa.[10] By labeling aluminum oxide microplatelets with iron oxide nanoparticles to exhibit an ultrahigh magnetic response (UHMR),[11] it should be possible to locally increase the elastic modulus of polyurethane substrates up to 300−500 MPa. Such values approach those typically achieved with standard flexible substrates (e.g., Kapton E, E = 5 GPa). Elastic moduli within this range would decrease the mechanical mismatch between stiff islands and the underlying elastic substrate, possibly increasing the lifetime of deposited thin film devices.

In this letter, we report the use for the first time of a particle-reinforced polymer-based composites as elastic substrates for the deposition of thin film devices for elastic electronic applications. Using magnetically responsive stiff alumina platelets as reinforcements of the polymer, we show that it is possible to form stiffer regions close to the composite surface to locally protect stiff electronic devices. Further, we demonstrate that the strengthened regions can be made sufficiently smooth to enable the patterning and successful operation of thin film transistors (Figure 1).

To demonstrate the potential of our approach in locally reinforcing substrates of various chemistries at the macro and microscales, we use a thermoplastic polyurethane elastomer (PU, Elastollan C64D, BASF), a silicone elastomer (PDMS, Sylgard 184, Dow Corning) and a cross-linked poly(vinyl alcohol) (PVA, 13 000−23 000 g/mol, 87−89% hydrolyzed, Sigma-Aldrich) as polymeric matrices. These three choices encompass three diverse polymer formulations that involve aqueous solvent (PVA), organic solvent (DMF), and solvent-free (PDMS) processes, allowing the generality of this method to be probed. Reinforcement of these substrates was achieved using 7.5 μm-long, 200 nm-thick alumina platelets as stiff, reinforcing elements (Alusion, Antaria, Australia Limited). To enable magnetic control of the reinforcing elements, the alumina platelets are coated with 0.1−1.0 vol% super-paramagnetic iron oxide nanoparticles. In a typical procedure, 8 g of alumina platelets are stirred in 200 mL of deionized water at pH 7, while 200 μL of EMG-705 ferrofluid (Ferrotec, Germany) is added dropwise. The 12 nm iron oxide particles in the ferrofluid are coated with an anionic surfactant, allowing for electrostatic binding to the positively charged platelets. A 1 h incubation period is sufficient to coat alumina platelets with the iron oxide nanoparticles. The water solution is rinsed three times and the platelets are then completely dried at 150 °C for 24 h.

Reinforced composites are produced by adding the magnetized alumina platelets to a fluid polymer (PU and PVA) or monomer (Sylgard 184) solution followed by mold casting and curing through either solvent evaporation or polymerization, respectively, in an oven at 60−80 °C. For proper transfer of stress from the softer matrices to the stiffer reinforcement particles during mechanical loading, a strong particle−matrix interface is crucial. PVA was found to naturally interact strongly with the magnetized platelets as shown by the increase in stiffness of 265% with the addition of 20 vol% platelets (Figure 2a). To enhance the interaction of PU with

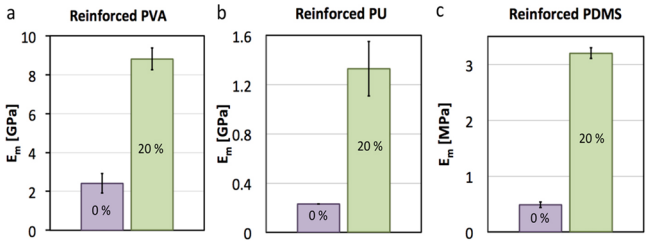

Figure 2. Measured Young's moduli for (a) PVA, (b) PU, and (c) PDMS without reinforcement (left bar) and with 20 vol% Al_2O_3 reinforcement platelets (right bar).

the platelets, the PU-Al_2O_3 composites were subjected to a postcuring heat treatment for 3 h at 120 °C. This increased the stiffness of the PU by 478% for 20 vol % platelets (Figure 2b). For PDMS substrates, a beneficial interaction between the particles and the PDMS matrix required hydrophobization of the alumina platelets. For hydrophobization, an initial coating of silica was first deposited on the alumina platelets. The silica coating of UHMR alumina platelets was performed by a modified Stöber method described earlier by Graf and co-workers[12] (for details, see the Supporting Information). To eventually hydrophobize the particles, we stirred 1 g of silica-coated platelets for 24 h in a 7 mL solution of isopropanol containing 150 mg of octadexyltrimethoxysilane (Acros, 90%) and 15 mg of n-butylamine (Sigma-Aldrich, 99.5%). The resulting hydrophobic magnetized platelets were found to increase the stiffness of the PDMS by 558% for 20 vol% platelets (Figure 2c). The stiffness of these materials was observed to increase linearly with the reinforcement particle concentration (for details, see the Supporting Information).

Macroscale local reinforcement of elastic substrates was achieved by applying a magnetic field gradient to the cast samples using the edge of a 5 cm × 5 cm × 2 cm rare earth magnet (Supermagnete, Switzerland), as indicated in Figure 3a. The magnetized alumina platelets were attracted to the magnetic field maximum near the edge of the magnet, leading to the formation of 5 mm-wide linear stripes with a high local concentration of reinforcing elements in the middle of a homogeneous nonreinforced matrix. Figures 3b,c show examples of PU and PDMS elastic substrates, respectively, in which a 5 mm-wide region is locally structured with alumina platelets.

Reinforcement of the polymer substrate at smaller length scales is also possible by using programmable magnetic tapes,

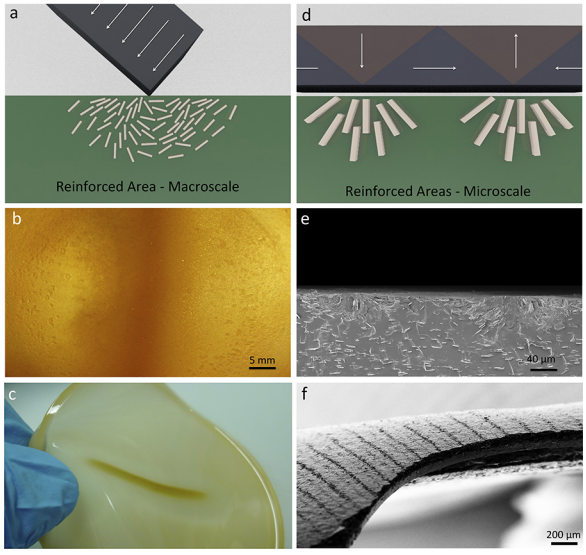

Figure 3. (a) Schematic and (b, c) photographs of a macroscale, locally structured substrate of (b) PU and (c) PDMS showing a spatial gradient of alumina reinforcing platelets in a polymer that leads to local stiffening (dark brown region). (d) Schematic and SEM (e) cross-section and (f) top-view of a microscale locally structured substrate showing 40 μm patterned regions of alumina reinforcing platelets in both (e) PVA and (f) PU using easily programmable magnetic tapes.

Figure 3d. To achieve substrates with local islands of reinforcement of both PVA and PU films with spatial resolution down to 20 μm, a programmed magnetic field pattern was applied using a magnetic tape containing magnetic domains with a periodicity of 150 μm. Such linear microdomains led to regions of locally concentrated platelets with widths of 30 μm, as shown in Figure 3e,f for PVA and PU elastic substrates, respectively. Although there exists significant interest for flexible electronics at such large size scales, it is important to note that the method proposed in this work is also scalable to smaller dimensions even by a few orders of magnitude.

In this work, we primarily focus on concentrating the reinforcement at a surface, as this allows the region under the reinforced island to remain ductile. However, if graded stiffness is required throughout the material thickness, then symmetric magnetic sources below and above the material may be used. Finally, the depth of penetration of the magnetic localization of reinforcement is dependent only upon the employed field sources as the resulting material has negligible susceptibility. With standard permanent magnets, penetration depths are on the scale of a few centimeters.

To evaluate if the accumulation of platelets in specific regions of the polymer is effective in locally reinforcing the elastic substrate, we performed mechanical tensile tests on samples extracted from substrates with macroscale reinforcement (Figure 3a). The 100–200 μm thick dogbone samples were cut along the long-axis of the macroscale reinforced area and had active tensile areas of 12 mm × 2 mm (Figure 4a). Tensile tests were conducted using an Instron 4411 Universal Testing Machine at a constant strain rate of 10 mm/minute. A cross-section of the reinforced region of the fractured polyurethane substrate clearly shows the desired local bilayer structure in the film (Figure 4b). In these samples, the alumina platelets are pulled into this bilayer due to the magnetic field gradient arising from the permanent magnet that is further aided by

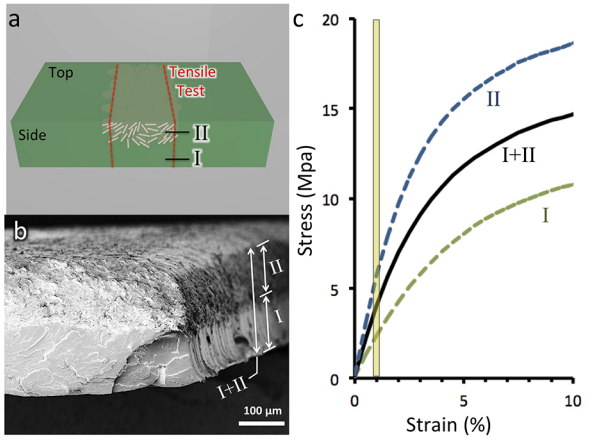

Figure 4. (a) Schematic depicting the tensile test region (red) within the locally reinforced substrates. (b) Scanning electron micrograph of the cross section of the reinforced region showing the bilayer structure. (c) Typical stress–strain curves for the measured bilayer PU substrates (black), for pure PU polymer substrate (green), and for the calculated reinforced regions on which TFT devices are to be patterned (blue). The highlighted region indicates the "danger zone" between 0.7 and 1% tensile strain where we expect TFT device failure.

gravitational sedimentation. The average tensile elastic modulus of the bilayered reinforced region within the polyurethane sample is found to be 333 MPa compared to the modulus of the pure polyurethane at 230 MPa (Figure 4c). Classic bilayer theory can be used to estimate the moduli of the reinforced layer alone. The Young's modulus of the bilayer, E_{net}, can be determined with a rule of mixtures as

$$E_{net} = \phi_I E_I + (1 - \phi_I) E_{II} \quad (1)$$

where ϕ is volume fraction, II refers to the reinforced layer containing the alumina particles, and I refers to the pure polyurethane layer (Figure 4). The volume fraction of I is determined from Figure 4b to be $\phi_I = 0.50$. Taking an elastic modulus, E_I, equal to 230 MPa for the nonreinforced polyurethane layer,[10,11] we can assume a Young's modulus, E_{II}, of 420–450 MPa for the reinforced layer (Figure 4c). This shows an increased stiffness of 190% compared to the pure polyurethane. Such increase in modulus means that the reinforced region will experience 52.8% of the strain of the nonreinforced polyurethane. This should allow the reinforced substrate to strain globally 2% for a local strain in the reinforced region of approximately 1%. Although the reinforcement obtained in this proof-of-concept example is not yet high enough to allow for extensive stretching of the substrate without reaching critical strain levels in the island, optimization of the platelet/matrix interfacial bonding and the local concentration of reinforcing particles should lead to much higher reinforcement levels[10] and global to local strain ratios, as suggested by the effective reinforcement demonstrated in homogeneous samples (Figure 2).

Given the submicrometer thicknesses of the inorganic layers of thin film devices, the surface roughness of the polymer substrate has to be sufficiently low to obtain defect-free layers after standard photolithography. To evaluate if the roughness of typical platelet-reinforced composites is sufficiently low for patterning and successful operation of thin film devices, we investigated fabricating thin film transistors (TFTs) on the surface of polyurethane substrates homogeneously reinforced with 20 vol % alumina platelets. Using atomic force microscopy

(AFM), we measured a surface roughness of around 200 nm in the homogeneously reinforced substrates, as opposed to values in the range 125 nm for the pure polymer obtained under the same processing conditions.

TFTs were fabricated on the homogeneously reinforced substrate using a bottom-gate inverted staggered geometry. For a schematic of the TFT device structure, refer to Cherenack et al.[13] Figure 5a shows the TFT channel region fabricated on the

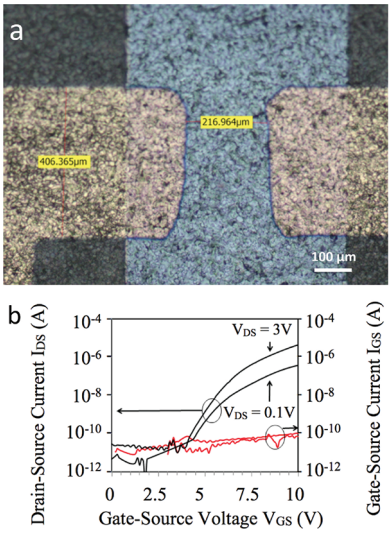

Figure 5. (a) Micrograph of an elastic TFT channel region for a device fabricated on a stiffened substrate, (width/length ≈ 400 μm/200 μm). (b) Associated transfer characteristic of the TFT deposited on a homogeneously reinforced elastic substrate.

reinforced substrate. All thin film layers were deposited and patterned via shadow masking. First, a 5 nm/50 nm/5 nm Ti/Au/Ti metal trilayer was deposited to form the gate electrodes using a Univex500 thermal evaporator. The next step involved deposition of TFT islands consisting of 63 nm Al_2O_3 (deposited using atomic layer deposition in a Picosun Sunale R-150B at 120 °C) and 15 nm IGZO (deposited using RF sputtering at room temperature). Finally, a second 5 nm/50 nm/5 nm Ti/Au/Ti metal trilayer was deposited to form the source/drain electrodes. The TFT channel width/length was designed to be approximately 400 μm/200 μm (see the image of a TFT channel region in Figure 5). All TFTs under test were characterized using a Keithley SCS4200 parameter analyzer connected to a Süss PM8 wafer prober. We obtained the transfer characteristics of TFTs by measuring the drain-source current (I_{DS}) as a function of the gate-source voltages (V_{GS}), which was varied from 0 to 10 V while setting the drain-source voltage (V_{DS}) at 0.1 and 3 V. The measured transfer characteristic in Figure 5b was used to extract the linear mobility, the saturation mobility, the subthreshold slope and the threshold voltage using standard equations to model the TFT current.[14]

With a yield of 11%, the first TFT results are promising, showing a linear mobility of 9.36 $cm^2/(V\ s)$, a saturation mobility of 4.59 $cm^2/(V\ s)$, a subthreshold slope of 1.4 V/decade, a threshold voltage of 7 V and an on/off ratio of 1×10^5. This can be compared to state-of-the art TFTs with measured linear mobilities of around 9 cm^2/Vs, saturation mobilities of around 8−9 cm^2/Vs, threshold voltages <0.5 V, and on/off ratios of around 1×10^6.[14] The high surface roughness of the substrate was likely the main reason for the low yield of functional TFTs. With optimized processing techniques, surface roughness can be reduced to greatly increase transistor production yield.

In summary, this work shows that it is possible to fabricate high-performance rugged TFTs on particle-reinforced composites with locally tuned mechanical properties. Local reinforcement of a variety of polymer substrates including PU, PDMS, and PVA, was demonstrated at the macro- and microscales using magnetized alumina platelets as reinforcing elements. Scalability of the reinforcing features can be achieved by using smaller size-scale magnetic gradients such as those from programmable magnetic tapes. Finally, we have shown that the typical roughness of the proposed particle-reinforced composites is sufficiently low to enable the patterning and successful operation of the first thin film transistors on alumina-reinforced polyurethane with performance comparable to that of state-of-the-art devices.

■ ASSOCIATED CONTENT

Supporting Information

The procedure to coat Ultra-High Magnetic Responsive (UHMR) alumina platelets with silica, the surface characterization of the resulting coated platelets, and the elastic modulus of polymer-based composites as a function of the concentration of alumina platelets. This material is available free of charge via the Internet at http://pubs.acs.org.

■ AUTHOR INFORMATION

Corresponding Author

*E-mail: andre.studart@mat.ethz.ch.

Author Contributions

‡These authors contributed equally to this work.

Notes

The authors declare no competing financial interest.

■ ACKNOWLEDGMENTS

The authors thank Dr. Christopher Simone from DuPont for his support, Mr. Frieder Reusch and Mr. Alain Reiser for their experimental work, the Swiss National Science Foundation (grant 200021_135306) for funding, Antaria and Merck for kindly supplying the alumina platelets, and the Electron Microscopy Center of ETH Zurich (EMEZ) for their support on the SEM and EDX analyses.

■ REFERENCES

(1) Kim, D. H.; Viventi, J.; Amsden, J. J.; Xiao, J. L.; Vigeland, L.; Kim, Y. S.; Blanco, J. A.; Panilaitis, B.; Frechette, E. S.; Contreras, D.; Kaplan, D. L.; Omenetto, F. G.; Huang, Y. G.; Hwang, K. C.; Zakin, M. R.; Litt, B.; Rogers, J. A. *Nat. Mater.* **2010**, *9*, 511−517.

(2) Viventi, J.; Kim, D. H.; Moss, J. D.; Kim, Y. S.; Blanco, J. A.; Annetta, N.; Hicks, A.; Xiao, J. L.; Huang, Y. G.; Callans, D. J.; Rogers, J. A.; Litt, B. *Sci. Transl. Med.* **2010**, *2*, 24ra22.

(3) Ko, H. C.; Stoykovich, M. P.; Song, J. Z.; Malyarchuk, V.; Choi, W. M.; Yu, C. J.; Geddes, J. B.; Xiao, J. L.; Wang, S. D.; Huang, Y. G.; Rogers, J. A. *Nature* **2008**, *454*, 748−753.

(4) Lacour, S. P.; Jones, J.; Wagner, S.; Li, T.; Suo, Z. G. *Proc. IEEE* **2005**, *93*, 1459−1467.

(5) Ryhanen, T. Future of Mobile Devices−Energy Efficient Sensing, Computing, and Communication. In *Proceedings of the 2009 Symposium on VSLI Circuits*; IEEE: Piscataway, NJ, 2009; pp 80−83

(6) Sekitani, T.; Nakajima, H.; Maeda, H.; Fukushima, T.; Aida, T.; Hata, K.; Someya, T. *Nat. Mater.* **2009**, *8*, 494−499.

(7) Gonzalez, M.; Axisa, F.; Bossuyt, F.; Hsu, Y. Y.; Vandevelde, B.; Vanfleteren, J. *Circuit World* **2009**, *35*, 22−29.
(8) Sekitani, T.; Noguchi, Y.; Hata, K.; Fukushima, T.; Aida, T.; Someya, T. *Science* **2008**, *321*, 1468−1472.
(9) Cotton, D. P. J.; Popel, A.; Graz, I. M.; Lacour, S. P. *J. Appl. Phys.* **2011**, *109*, 054905.
(10) Libanori, R.; Münch, F. H. L.; Montenegro, D. M.; Studart, A. R. *Compos. Sci. Technol.* **2012**, *72*, 435−445.
(11) Erb, R. M.; Libanori, R.; Rothfuchs, N.; Studart, A. R. *Science* **2012**, *335*, 199−204.
(12) Graf, C.; Vossen, D. L. J.; Imhof, A.; van Blaaderen, A. *Langmuir* **2003**, *19*, 6693−6700.
(13) Cherenack, K. H.; Munzenrieder, N. S.; Troster, G. *IEEE Electron Device Lett.* **2010**, *31*, 1254−1256.
(14) Neamen, D. A., *Semiconductor Physics and Devices: Basic Principles*; McGraw-Hill: New York, 2003.